Journal of Controlled Release 289 (2018) 102–113

Contents lists available at ScienceDirect

Journal of Controlled Release

journal homepage: www.elsevier.com/locate/jconrel

Cell-permeable NF-κB inhibitor-conjugated liposomes for treatment of glioma

Yanyu Zhang[a,1], Li Zhang[a,1], Yang Hu[a], Kuan Jiang[a], Zhuoquan Li[b], Yao-Zhong Lin[b,c], Gang Wei[a,*], Weiyue Lu[a]

[a] Key Laboratory of Smart Drug Delivery, Ministry of Education & PLA, Department of Pharmaceutics, School of Pharmacy, Fudan University, Shanghai 201203, China
[b] The Institute for Biomedical Engineering & Nano Science, Tongji University School of Medicine, Shanghai 200092, China
[c] Celtek Bioscience, LLC, 2550 Meridian Boulevard, Suite 200, Franklin, TN 37067, USA

ARTICLE INFO

Keywords:
CB5005
NF-κB inhibitor
Cell-penetrating peptides
Liposomes
Glioma

ABSTRACT

Application of liposomes-based drug delivery in treatment of glioma has been hampered by the poor permeability of blood-brain barrier and the low uptake efficiency by glioma tissues. Moreover, many chemotherapy drugs promote the activation of the NF-κB, which plays a role in the development and progression of cancer and chemoresistance. In this report, CB5005 peptide, designed for its dual function in cell membrane penetration and NF-κB inhibition, was conjugated to PEGylated liposomes loaded with doxorubicin (CB5005-LS/DOX) or a fluorescent dye (CB5005-LS/dye). These CB5005-modified liposomes were utilized for targeting and penetrating glioma. Both qualitative and quantitative evaluations of CB5005-LS/dye showed that modification by CB5005 significantly increased cellular uptake of the liposomes by glioma cells, and substantially improved permeability of the liposomes into tumor spheroids. Intracellular localization studies demonstrated that CB5005-modified liposomes could not only penetrate into glioma cells but also deliver DOX into the nucleus. Cytotoxicity assay indicated that compared with the unmodified DOX liposomes (LS/DOX), CB5005-LS/DOX increased the efficiency of killing glioma cells by more than fivefold. *In vivo* imaging illustrated that CB5005-modified liposomes, *via* intravenous injection, distributed fluorescence into the brain and accumulated at tumor xenograft and intracranial glioblastoma in different animal models. More importantly, CB5005-LS/DOX treatment significantly prolonged the survival time of nude mice bearing intracranial glioblastoma. In summary, CB5005-modified liposomes represent a promising drug delivery system for cancer treatment attributing to its unique ability not only to transfer drugs to the tumor sites but also to function as a synergist for chemotherapy of glioma and other human tumors.

1. Introduction

Glioma is one of the major tumors that threaten people's lives for the rapid progression and poor prognosis though the dramatic development of medical technology in the last decade [1]. The current treatments of glioma include surgical resection, radiotherapy and chemotherapy [2]. However, it is almost impossible for surgical resection and/or radiotherapy to remove tumor tissue completely without affecting normal brain functions due to lack of sharp border of glioma [3–5]. Reasonable chemotherapy remains a primary tool for glioma treatment [6,7]. Unfortunately, poor site-specific delivery, incapable deep-penetration into tumor, and the formidable challenge of delivering therapeutic agents to brain due to existence of blood-brain barrier (BBB) and blood-brain tumor barrier (BBTB) are the intrinsic limitations to successful chemotherapy [8,9]. One promising solution for delivering therapeutic molecules across the BBB, BBTB and even penetrating into tumor is to use cell-penetrating peptides (CPPs) [9–11], which showed the potential in developing drug delivery technologies for brain disorders, such as brain glioma [12].

CPPs have been utilized as a powerful tool for intracellular delivery of various therapeutic molecules and have received extensive attention in recent decades [13–15]. Most of these CPPs were defined as short cationic peptides consisting of < 30 amino acids with attractive capability of cellular uptake without causing severe cytotoxicity [16–19]. CPPs and their conjugated cargoes translocate through cell membrane *via* direct penetration, formation of inverted micelles or transient pores,

* Corresponding author.
E-mail address: weigang@shmu.edu.cn (G. Wei).
[1] Equally contributing authors.

https://doi.org/10.1016/j.jconrel.2018.09.016
Received 7 April 2018; Received in revised form 5 August 2018; Accepted 19 September 2018
Available online 20 September 2018

macropinocytosis, endocytosis mediated by clathrin or caveolae [20]. The typical examples of CPPs are naturally originated Tat (48–60 residues derived from human immunodeficiency virus) [21] and cationic peptide oligoarginine [22]. However, these kinds of CPPs are deficient in accumulation at tumor site due to lack of tissue selectivity and tumor-targeting ability [23,24]. CPPs and their conjugated cargoes are readily to be internalized by nearly all kinds of cells and are prone to accumulate at the organs with abundance of blood capillaries, such as liver and kidney [25,26]. Moreover, most of CPPs are readily to be eliminated by the reticuloendothelial system due to high electro-positivity, which makes CPPs easy to interact with those negatively charged components in plasma. Therefore, the clinical application of CPPs in tumor therapy has been greatly restricted [27–29].

Many artificially designed and synthesized CPPs were emerged to improve the delivery efficiency and tumor-targeting ability of therapeutic agents [30–32]. CB5005, developed by Celtek Bioscience [33], is a peptide with excellent cell and nucleus permeability. It is composed of 21 amino acid residues, which can be divided into two cascaded segments: an 11-residue membrane-permeable sequence and a 10-residue nuclear localization sequence [34,35]. There are only two basic lysine residues in the membrane-permeable sequence of CB5005 peptide, which differs from the traditional CPPs for its weak electro-positivity. As a result of this design, CB5005 has displayed its unique capabilities of BBB penetration and tumor accumulation, as we reported recently [33].

Nuclear factor-κB (NF-κB), a family of transcription factors, regulate multiple processes in cells, which involve cell survival, proliferation, differentiation and cytokine production. NF-κB family consists of five proteins, including p50, p52, p65 (Rel A), c-Rel and RelB [36,37]. In the state of inactivation, NF-κB is combined with IκB proteins in cytoplasm. Once being stimulated, IκB is phosphorylated by IκB kinase, leading to ubiquitination and proteasomal degradation. This triggers the formation of NF-κB dimmers, which actively shuttle between the nucleus and cytosol, then stay in nucleus and induce gene expression [38]. Activation of NFκB is rapidly and transiently induced by many factors, such as viral and bacterial infections, DNA damage and proinflammatory cytokines. Notably, it was found that NFκB was constitutively activated in most malignant cells and in the tumor microenvironment [37,39]. The nuclear localization sequence of CB5005 is derived from p50 subunit, which can competitively prevent the translocation of NF-κB into nucleus and act as a blocking agent of NF-κB [40]. We previously demonstrated that when applied with doxorubicin, CB5005 showed a synergistically antagonistic effect on glioma [33].

Nanoscale drug delivery systems have exhibited distinct advantages over traditional formulations in tumor treatment [41–43]. Among these delivery systems, liposomes have gained more and more attention over the past three decades for their unique characteristics, including biocompatibility, biodegradability, low toxicity, lack of immune system activation and capability to incorporate both hydrophilic and hydrophobic drugs [44]. Moreover, surface-functionalized liposomes have been widely applied to target specific cancer cells and transfer cargoes to cytoplasm efficiently [45,46].

In the present study, CB5005 was conjugated to a PEGylated liposomal carrier to facilitate the glioma treatment of antineoplastic agent doxorubicin (DOX) (CB5005-LS/DOX). The permeability of CB5005-LS/X (here X represents DOX or a fluorescence probe) at cellular and tumor spheroid level was going to be evaluated and compared with unmodified liposomes (LS/X). Intracellular localization of the liposomes would also be observed to illustrate their potential in nuclear delivery of DOX. The *in vitro* cytotoxicity of CB5005-LS/DOX would be investigated and compared with LS/DOX in glioma cells. Then, the *in vivo* distribution of CB5005-LS/X would be assayed after intravenous injection in normal mice, xenografts-bearing mice, and intracranial glioblastoma-bearing mice, respectively. Finally, the therapeutic efficacy of CB5005-LS/DOX to intracranial glioblastoma-bearing mice would be investigated.

2. Materials and methods

2.1. Materials

CB5005-Cys, which amino acid sequence is KLKLALALALAVQRKRQKLMPC, was synthesized by China Peptides Co., Ltd. (Shanghai, China). The purity and molecular mass of the peptide were verified by high performance liquid chromatography (HPLC) and electro-spray ionization mass spectrometry (ESI-MS), respectively. Maleimide-derivatized polyethylene glycol 3400-distearyl phosphatidylethanolamine (Mal-PEG_{3400}-DSPE) was purchased from Laysan Bio Co., (Arab, USA). Hydrogenated soybean phosphatidylcholine (HSPC) and methoxyl-PEG 2000-DSPE ($mPEG_{2000}$-DSPE) were purchased from Lipoid GmbH (Ludwigshafen, Germany). Cholesterol was purchased from Sinopharm Chemical Reagent Co., Ltd., (Shanghai, China). Sephadex G-50 and 5-carboxyfluorescein (FAM) was purchased from Sigma (St. Louis, USA). 1,1′-dioctadecyl-3,3,3′,3′-tetramethyl indotricarbocyanine iodide (DiR) was purchased from Invitrogen (Carlsbad, USA). Doxorubicin (DOX) was obtained from Huafeng United Technology Co., Ltd. (Beijing, China). 4′,6-diamidino-2-phenylindole (DAPI) was supplied by Roche (Switzerland). 1,1′- dioctadecyl-3,3,3′,3′-tetramethylindodicarbocyanine perchlorate (DiD) was purchased from Meilune (Dalian, China).

Human glioma cells U87 were purchased from Cell Bank, Chinese Academy of Sciences (Shanghai, China). Dulbecco's modified Eagle's medium (DMEM), fetal bovine serum (FBS), 0.25% trypsin-EDTA, agarose and penicillin-streptomycin were purchased from Gibco (Carlsbad, USA). 3-(4,5-dimethyl-2-thiazolyl)-2,5-diphenyl-2-H-tetrazolium bromide (MTT) was obtained from Amresco (Solon, USA). Cell culture plate and flask were purchased from Coring (Oneonta, USA). All chemicals were analytic reagent grade.

Male nude mice, weighing 20 g, were purchased from Shanghai SLAC Laboratory Animal Co., Ltd. (Shanghai, China) and kept under specified pathogen free conditions. All animal experiments were performed in accordance with guidelines evaluated and approved by the Ethics Committee of Fudan University.

2.2. Western blot analysis

Western blot analysis was performed to evaluate the effect of CB5005 on the NF-κB pathway in glioma cells. Briefly, U87 cells were incubated with CB5005 at different concentrations ranging from 5 μM to 50 μM for 48 h. Whole cytoplasmic proteins and nuclear proteins were extracted using Nuclear and Cytoplasmic Protein Extraction Kit (Beyotime, Shanghai, China). Quantified nuclear protein lysates were separated by 10% polyacrylamide SDS-PAGE gels and then transferred to PVDF membranes (Millipore, Billerica, USA). The membranes were probed with p50 and Histone 3 antibodies, which were purchased from Cell Signaling Technology (Danvers, USA). The proteins were visualized using an enhanced chemiluminescence Western blot detection system (Bio-Rad, Hercules USA).

2.3. Synthesis and characterization of functionalized membrane material

CB5005-PEG_{3400}-DSPE was synthesized by conjugating the cysteine residue at the C-end of CB5005 to Mal-PEG_{3400}-DSPE. Briefly, one aliquot of CB5005-Cys buffer solution was mixed with two aliquots of Mal-PEG_{3400}-DSPE dimethyl formamide (DMF) solution at a molar ratio of 1.2:1. Then the mixture was gently stirred for 2 h at room temperature. The product was purified by dialysis (MWCO 3.5 kDa, Millipore, USA) against ultrapure water at the endpoint of the reaction. The dialysate containing CB5005-PEG_{3400}-DSPE was analyzed by HPLC (Agilent 1100 series, USA) and nuclear magnetic resonance (NMR, Varian, USA), and finally was freeze-dried (Alpha2–4, Martin Christ, Germany).

2.4. Preparation of liposomes

Liposomes loading with DOX, fluorescent probe FAM or DiR were prepared by the thin-film hydration and extrusion method as reported procedure [47,48]. A mixture of HSPC/Cholesterol/mPEG$_{2000}$-DSPE/CB5005-PEG$_{3400}$-DSPE (liposomes with the modification of CB5005, 52:43:3:2, molar ratio) or HSPC/Cholesterol/mPEG$_{2000}$-DSPE (liposomes without modification, 52:43:5, molar ratio) in 5 mL $CHCl_3$ was rotary evaporated to form thin film, which was then vacuum desiccated overnight. For DOX-loaded liposomes, an ammonium sulfate gradient method was adopted to load DOX into the liposomes [49,50]. That is, the thin film was hydrated using 0.32 M ammonium sulfate solution with oscillator at 60 °C water bath for 2 h. The resulting solution was extruded through a series of polycarbonate membranes (Whatman, USA) with the pore size ranging from 200 nm down to 50 nm using a mini-extruder (Avanti, USA). The external ammonium sulfate was replaced by normal saline solution through a Sephadex G-50 column. The ammonium sulfate liposomes were mixed with 5 mg/mL DOX in normal saline solution at the weight ratio of 1:10 and shaken for 30 min under 60 °C. Then, the liposomes were separated from free DOX on a Sephadex G-50 column which was equilibrated with normal saline. DOX concentrations in the liposomal samples were measured with the ultraviolet spectrophotometer at 480 nm following dissolution in 5% Triton solution (UV-2401PC, Shimadzu, Japan). The morphology of liposomes was characterized by a transmission electron microscopy (TEM). In the meantime, the size of liposomes was determined at 25 °C by the dynamic light scattering method (Malvern Zetasizer 3000).

FAM-loaded liposomes were prepared with the similar procedure as mentioned above, except that the hydration medium was FAM solution instead of ammonium sulfate solution. DiR-loaded liposomes were prepared with the similar method of FAM-loaded liposomes, except that DiR was mixed with the membrane materials in the chloroform solution at the beginning, and the thin film was hydrated using normal saline. All the procedures were proceeded in darkness.

2.5. In vitro leakage of DOX

The *in vitro* leakage of DOX from the liposomes was investigated by dialysis method in phosphate buffer (pH 7.4) or serum at 37 °C as previously reported [51]. The concentrations of DOX were determined by a fluorescence spectrophotometer (Cary Eclipse, Agilent, Australia) at Ex/Em 494/522 nm.

2.6. Cellular uptake

The human glioma cells U87 harvested at the logarithmic growth phase were seeded in confocal dishes with a density of 5000 cells/well and incubated for 24 h with 5% CO_2 at 37 °C in a Heraueus incubator (Kendro, USA). The cells were incubated with CB5005-LS/FAM, LS/FAM or FAM solution in the culture medium with 10% FBS for 4 h at a concentration of 1 μM FAM, then rinsed with phosphate buffered saline (PBS, pH 7.4) thrice, fixed with 4% paraformaldehyde (m/v) for 15 min, stained with 1 μg/mL DAPI for 10 min and moisturized with 50% glycerol (*v*/v). After that, the treated cells were observed with a laser scanning confocal microscope (LSCM, SP5, Leica, Germany). FAM fluorescence was excited with 488 nm wavelength of an argon laser and the emission was detected in a range of 500–540 nm.

For quantitative analysis of the cellular uptake of the liposomes, the U87 cells were harvested and seeded on 12 well plates at a density of 5×10^4 cells/well and incubated for 24 h. Then, the cells were respectively incubated with CB5005-LS/FAM, LS/FAM or FAM solution for 4 h at the concentrations of 1 μM, 0.1 μM and 0.01 μM FAM in the culture medium with 10% FBS. Afterwards, the cells were rinsed with PBS thrice, trypsinized with EDTA-trypsin, collected in the Eppendorf tubes and centrifuged at 1000 rpm for 5 min. The precipitated cells were subsequently re-suspended in 200 μL PBS and analyzed using a flow cytometer (FACSAria, BD, USA).

2.7. Tumor spheroid penetration

For further evaluation of the tumor-penetrating ability of the CB5005-LS/FAM, U87 cells at the logarithmic growth phase were seeded in 48-well plates (2000 cells/400 μL per well) which were precoated with 150 μL of 2% (*w/v*) low-melting-temperature agarose to prepare the three-dimensional tumor spheroids. After that, the plates were shaken gently to make the U87 cells gather together to form tumor spheroids and incubated for a week. Afterwards, the tumor spheroids with good morphology were incubated with CB5005-LS/FAM, LS/FAM and FAM solution for 4 h at a concentration of 1 μM FAM. The spheroids were then rinsed with PBS thrice before being fixed with 4% (m/v) paraformaldehyde for 15 min and observed with a LSCM as described above.

2.8. Intracellular localization analysis

Human glioma cells U87 were harvested at the logarithmic growth phase and seeded in confocal dishes with a density of 5000 cells/well and incubated for 24 h. Then U87 cells were incubated with CB5005-LS/DOX, LS/DOX or DOX solution at a concentration of 1 μM DOX for 4 h. After that, U87 cells were treated and observed with a LSCM at 480 nm.

2.9. Cell livability assay

The *in vitro* anti-tumor activity of DOX-loaded liposomes was determined by MTT assay. U87 cells at the logarithmic growth phase were seeded in 96-well plates at a density of 5000 cells/200 μL culture medium per well. Following attachment for 24 h, the culture medium in each well was replaced with 200 μL of fresh medium containing serial dilutions of CB5005-LS/DOX or LS/DOX ranging from 0.025 μM to 409.6 μM DOX. Each concentration was performed with triple wells. The cells were incubated with CB5005-LS/DOX or LS/DOX for 4 h and subsequently rinsed with PBS and incubated with culture medium for a total of 72 h before assessing cell livability. After that, 20 μL of 5 mg/mL MTT dissolved in PBS was added to each well directly. The plates were incubated for an additional 4 h and then the medium was discarded. Thereafter, 200 μL of dimethyl sulfoxide (DMSO) was added to each well to dissolve the formazan crystals while vigorously shaking the plates with an automated shaker for about 10 min. The absorbance of each well was measured on a micro-plate reader (Bio-Rad 680, USA) at a detection wavelength of 490 nm and the percentage of cell livability was calculated.

2.10. In vivo distribution in normal nude mice

In order to assess whether the liposomes modified with CB5005 are able to distribute in brain or not, nude mice were injected with 100 μL CB5005-LS/DiR or LS/DiR at a concentration of 0.01 μM DiR through tail vein, and normal saline was designated as negative control ($n = 3$). The mice were anesthetized with isoflurane and observed by a Xenogen *in vivo* imaging system (IVIS) coupled with Living Image software (Alameda, CA). At 4 h post administration when the intensity of fluorescence reached the peak value in brain, the mice were perfused with normal saline to remove the blood and fixed with 4% paraformaldehyde (m/v). Distribution of the liposomes in organs including heart, liver, spleen, lung, kidney and brain was immediately observed using the Xenogen IVIS spectrum.

2.11. In vivo distribution in xenografts-bearing nude mice

Nude mouse model bearing U87 xenografts was built by subcutaneous injection of approximate 2×10^6 U87 cells suspended in 100 μL of serum-free medium at right armpit to evaluate the *in vivo* tumor accumulation of CB5005-LS/DiR. Two weeks later, the tumor

volume was checked, and then the mice were treated with the DiR-containing liposomal formulations (3 mice in each group) and examined as the method mentioned above.

2.12. In vivo distribution in intracranial glioblastoma-bearing nude mice

Intracranial glioblastoma model was established in nude mice. Approximate 8×10^5 U87 cells were implanted into the right striatum (1.8 mm lateral to the bregma and 3 mm in depth) using a stereotactic fixation device equipped with a mouse adaptor (Stoteling, USA). After surgery, the mice were further maintained under standard housing condition for two weeks. Afterwards, the intracranial glioblastoma-bearing nude mice were treated with the DiR-containing liposomal formulations (3 mice in each group) and examined as mentioned above.

2.13. In vivo anti-glioblastoma efficacy

The survival time of intracranial glioblastoma-bearing nude mice treated with CB5005-LS/DOX was evaluated. The animal model was established as described above, and the glioblastoma-bearing mice were randomly divided into five groups (10 mice in each group) and separately treated with 100 μL of CB5005-LS/DOX, LS/DOX, DOX solution, blank CB5005-LS or normal saline at 10, 13, 16, 19, 22 days after implantation. The total dose of DOX to an individual mouse was 10 mg/kg body weight. The survival times of the mice were recorded and analyzed.

2.14. Statistical analysis

The IC_{50} values were calculated by nonlinear regression analysis with the software of GraphPad Prism. Differences between the treated groups in cellular uptake and the biodistribution were assessed using an unpaired Student's *t*-test. A p value $< .05$ was considered significant.

3. Results

3.1. Effect of CB5005 on NF-κB pathway in glioma cells

The expression level of NF-κB related protein p50 in the nuclei of human glioma cells and the effect of CB5005 on the NF-κB pathway were evaluated. According to the Western blot bands (Fig. 1A), we confirmed that NF-κB pathway was constitutively activated in U87 cells, which is consistent with the results recently reported by Pfeffer's group [52]. When incubated with CB5005 at the concentration above 40 μM, the quantified p50 protein level in the nuclei of U87 cells was significantly reduced ($p < .01$) compared with that in the untreated cells (Fig. 1B). This result manifested that CB5005 could competitively prevent NF-κB related protein from translocating into the nucleus and therefore block this intracellular pathway.

3.2. Characterization of functionalized membrane material

The HPLC spectra and NMR spectra of Mal-PEG_{3400}-DSPE and CB5005-PEG_{3400}-DSPE were shown in Fig. 2A. The retention time of Mal-PEG_{3400}-DSPE was 17.39 min when determined by HPLC. By contrast, the retention time of the synthetic product was 12.65 min, which was nearly 4 min ahead of Mal-PEG_{3400}-DSPE due to the increased hydrophilicity of CB5005-PEG_{3400}-DSPE. In the NMR spectrum of Mal-PEG_{3400}-DSPE, the maleimide had a characteristic peak at 6.7 ppm. However, this peak disappeared in the NMR spectrum of CB5005-PEG_{3400}-DSPE. Taken together, these results indicated that CB5005-PEG_{3400}-DSPE was synthesized successfully.

3.3. Characterization of liposomes

Characterizations of the DOX-loaded liposomes were summarized in Table 1. Modification by CB5005 slightly increased the particle size of the PEGylated liposome, which was about 110 nm with a polydispersity index < 0.2, as seen from the illustrated particle size distribution in Fig. 2B. TEM photographs showed that the liposomes LS/DOX and CB5005-LS/DOX were generally spherical and of regular shape (Fig. 2C). When CB5005 was modified on the liposomes surface, the zeta potential of CB5005-LS/DOX increased slightly from -8 mV to -5 mV due to the weakly positive charge of CB5005. Note that the zeta potential of CB5005-LS/DOX was still negative, which would benefit longer circulation time and therefore targeting distribution of the antineoplastic agent *in vivo*.

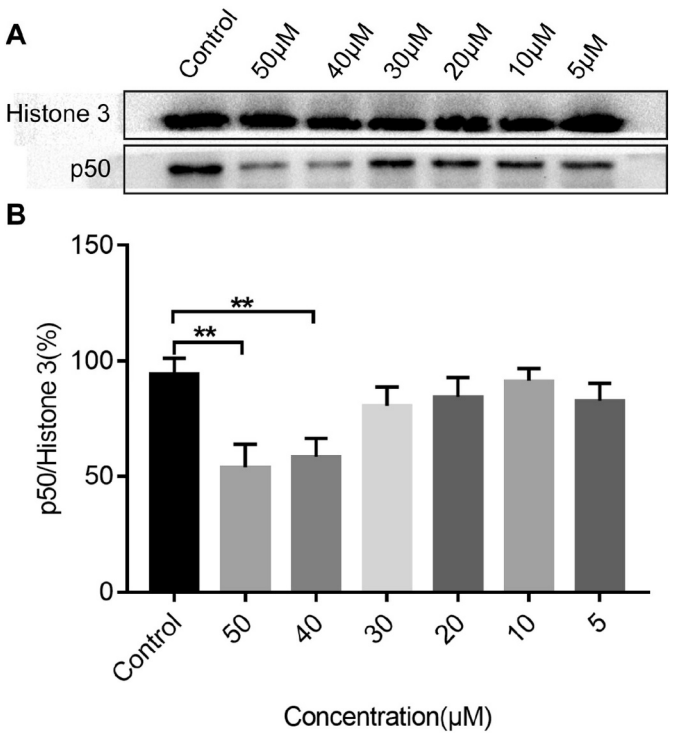

Fig. 1. Effect of CB5005 on nuclear protein p50 level in U87 cells. (A) Western blot bands. (B) Half-quantification of the p50 protein level. Data were presented as mean ± SD ($n = 3$). ** denotes statistical significance at a level of $p < .01$.

3.4. In vitro leakage of DOX

The liposomes with or without CB5005 modification exhibited similar release kinetics within 72 h against different media, as shown in Fig. 2D. Both of the liposomes were stable in PBS (pH 7.4), and only < 15% DOX was released in 72 h. By comparison, the release rate was significantly accelerated in serum, resulting in 50% DOX released from the liposomes during the same period. It seemed that introducing CB5005 on the outer surface of the liposomes had no influence on the *in vitro* DOX release.

3.5. Cellular uptake

Cellular uptake of CB5005-LS/FAM was qualitatively evaluated by confocal images of glioma cells U87, as shown in Fig. 3A. It was obvious that CB5005-LS/FAM could be efficiently internalized by U87 cells due to the cell-penetrating property of CB5005. Additionally, CB5005-LS/FAM could even deliver FAM into the nucleus of U87 cells due to the nuclear localization function of CB5005. In sharp contrast, LS/FAM and free FAM almost could not be internalized by U87 cells under the same circumstance.

Quantitative cellular uptake of CB5005-LS/FAM was subsequently confirmed by flow cytometry assay, as shown in Fig. 3B. The percentages of FAM-positive cells and mean value of cellular uptake displayed

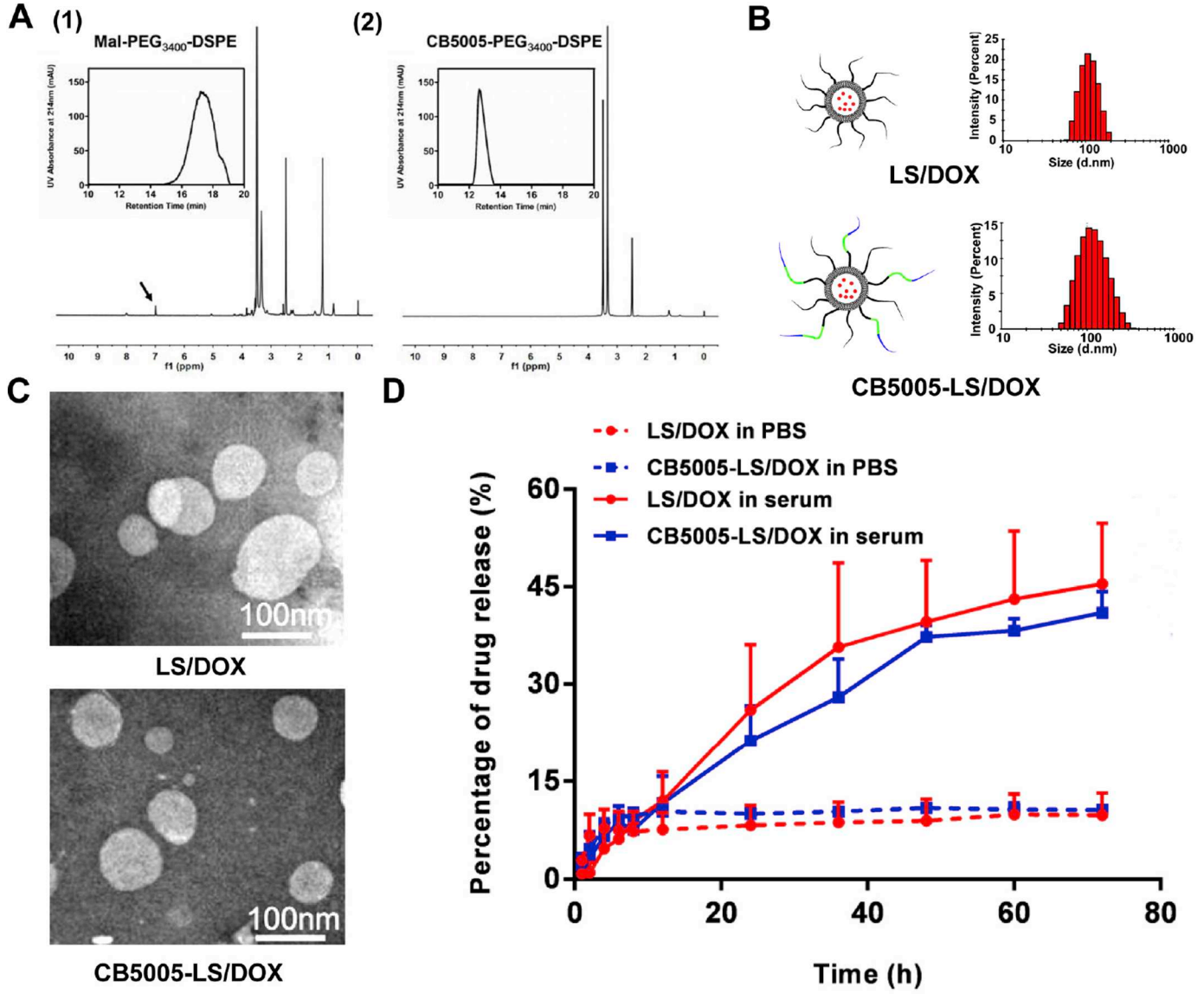

Fig. 2. Characterization of liposomes. (A) The HPLC spectra (upper) and NMR spectra (lower) of Mal-PEG$_{3400}$-DSPE (1) and CB5005-PEG$_{3400}$-DSPE (2). The characteristic peak of the maleimide in Mal-PEG$_{3400}$-DSPE was pointed out by the arrow. Size distribution (B) and TEM photographs (C) of LS/DOX and CB5005-LS/DOX. (D) Accumulative release of DOX from LS/DOX and CB5005-LS/DOX in PBS and serum.

Table 1
Characterization of the DOX-loaded liposomes without or with CB5005 modification (n = 3).

Formulation	Particle size (nm)	Polydispersity index	Zeta potential (mV)	Encapsulated efficiency (%)
LS/DOX	105.7 ± 0.35	0.054 ± 0.018	−7.97 ± 0.73	90.8 ± 2.0
CB5005-LS/DOX	111.7 ± 0.23	0.150 ± 0.034	−4.94 ± 0.99	70.0 ± 1.7

a tendency of increasing with incubation concentrations of the liposomes. Both of these two parameters were significantly higher ($p < .001$) when the cells were exposed to CB5005-LS/FAM under the concentrations ranging from 0.01 μM to 1 μM, compared with those cells exposed to LS/FAM or free FAM alone. Particularly, the FAM-positive percentage achieved > 99% for CB5005-LS/FAM treated cells even at the lowest incubation concentration of 0.01 μM, but was only < 1% for LS/FAM or free FAM treated cells under the same concentration.

3.6. Tumor spheroid penetration

Tumor spheroids were used to imitate the *in vivo* status of solid tumors and evaluate the permeability of CB5005-LS/FAM by confocal microscopy. As shown in Fig. 3C, the fluorescence intensity produced by CB5005-LS/FAM in the tumor spheroids was substantially higher than that in the other groups and almost no fluorescence could be observed in the tumor spheroids incubated with LS/FAM and free FAM. This result indicates that surface modification by CB5005 could effectively increase the tumor permeability of liposomes, which would play an important role in improving drug delivery.

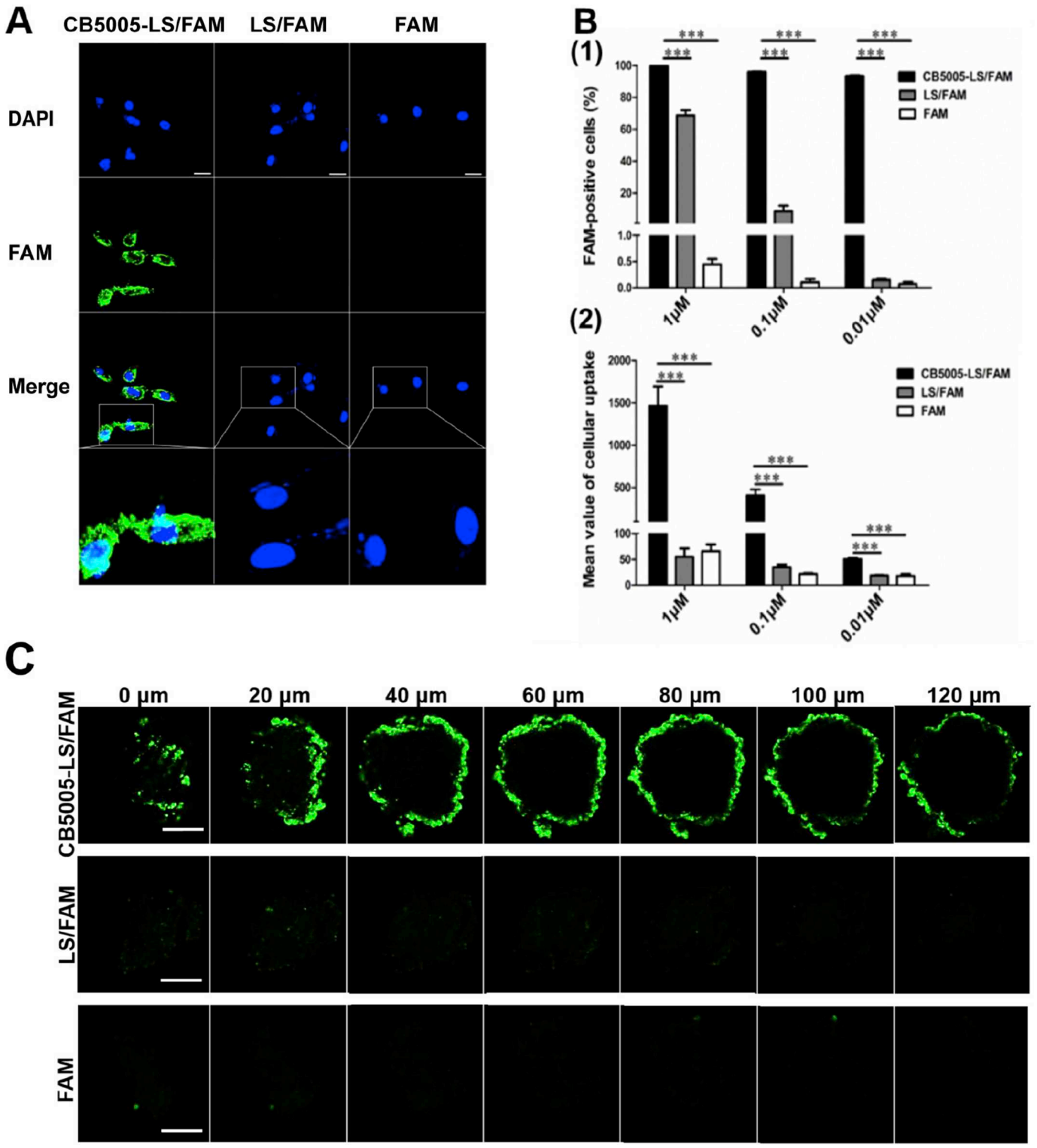

Fig. 3. Cellular uptake by U87 cells and permeability in U87 tumor spheroids. (A) Qualitative cellular uptake of CB5005-LS/FAM, LS/FAM and free FAM (equal FAM concentration at 1 μM) observed by confocal microscopy following incubation for 4 h. Scale bars = 30 μm. (B) Quantitative analysis on the percentage of FAM-positive cells (1) and the mean value of cellular uptake (2) determined by flow cytometry following incubation for 4 h. Data were presented as mean ± SD ($n = 3$). ***denotes statistical significance at a level of $p < .001$. (C) Penetration of CB5005-LS/FAM, LS/FAM and free FAM in U87 tumor spheroids at a concentration of 1 μM FAM. Images were taken by a confocal microscopy following incubation for 4 h. Pictures showed the fluorescent images of tumor spheroids from the bottom every 20 μm for 120 μm, bar represents 200 μm.

3.7. Intracellular localization analysis

DOX is a potent antitumor drug, which acts in the cell nucleus. Intracellular localization of DOX was visualized to elucidate if CB5005 modified liposomes could deliver DOX into the cell nucleus. As shown in Fig. 4A, CB5005-LS/DOX localized in the nucleus of U87 cells due to the nuclear localization sequence of CB5005. A similar distribution in the nucleus could be observed after free DOX was incubated with the

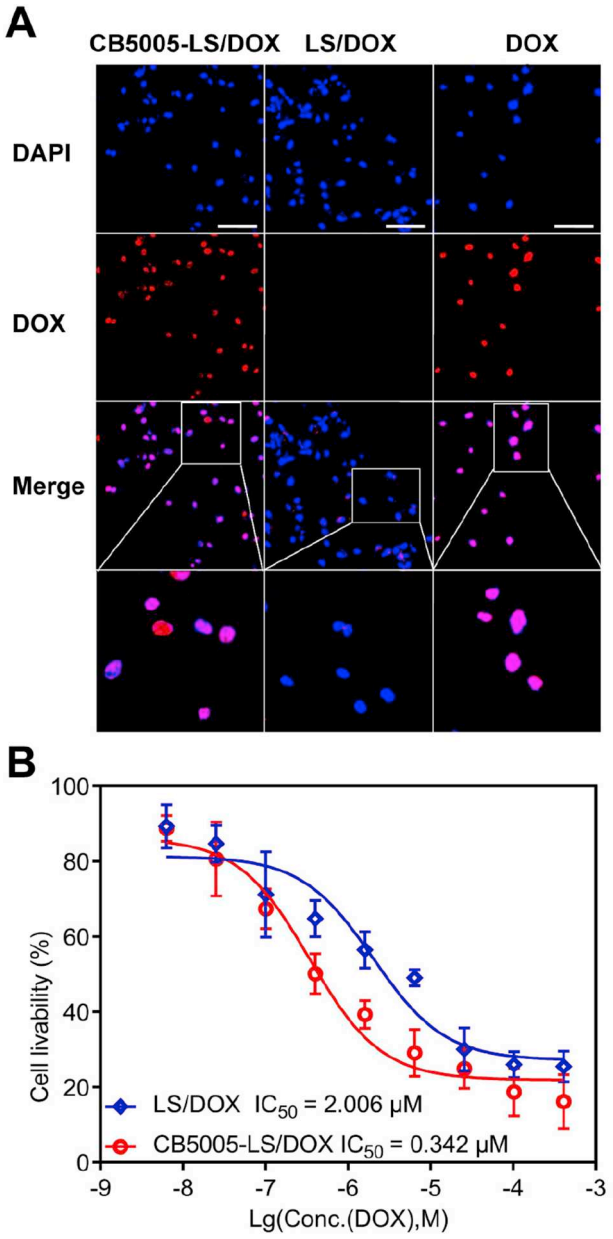

Fig. 4. Co-localization and cytotoxicity of liposomes loaded with DOX in U87 cells. (A) Intracellular localization of CB5005-LS/DOX, LS/DOX and free DOX in glioma cells U87 at the concentration of 1 μM. Images were taken on a confocal microscopy following a 4 h period of incubation. The nuclei were stained with DAPI (blue). Scale bar = 100 μm. (B) Concentration-dependent U87 cell viability curves after co-incubation with CB5005-LS/DOX and LS/DOX for 4 h determined *in vitro* by MTT assay ($n = 3$). (For interpretation of the references to colour in this figure legend, the reader is referred to the web version of this article.)

U87 cells. However, LS/DOX induced little uptake of DOX into the cytoplasm and nucleus of U87 cells after 4 h incubation. From the confocal imaging under higher magnification (Fig. S1), it could be clearly seen that DOX distributed in both cytoplasm and nucleus when the cells were treated with CB5005-modified liposomes. This result demonstrates that CB5005-LS/DOX could deliver DOX into the nucleus of glioma cells as effectively as free DOX.

3.8. Cell viability assay

The cytotoxicity of CB5005-LS/DOX and LS/DOX was detected on U87 cells. The IC_{50} (concentration leading to 50% cell-killing) of CB5005-LS/DOX and LS/DOX was determined from the concentration-dependent cell viability curves, as shown in Fig. 4B. The calculated IC_{50} of CB5005-LS/DOX was 0.342 μM. However, the calculated IC_{50} of LS/DOX was 2.006 μM, which was nearly six times higher than that of CB5005-LS/DOX. This result indicates that CB5005 modification could significantly increase the cytotoxicity of DOX liposomes.

3.9. In vivo distribution in normal nude mice

IVIS spectrum was used to study the distribution of CB5005-LS/DiR and LS/DiR in nude mice at 4 h post injection and normal saline was used as control. It was evident that CB5005 modification on the liposomal surface induced the highest *in vivo* brain distribution after intravenous injection when compared with LS/DiR and normal saline (Fig. 5A). *Ex vivo* images of dissected tissues including heart, liver, spleen, lung and kidney were also recorded with IVIS spectrum and the result showed that CB5005-LS/DiR and LS/DiR were widely distributed in the liver of the nude mice which is the major metabolic organ. The fluorescence intensity of brain was further quantified with the software of Living Image and the result showed that the fluorescence intensity of CB5005-LS/DiR-treated brain was significantly higher than that of LS/DiR ($p < .05$) and normal saline ($p < .001$) (Fig. 5B). This result indicates that CB5005 modified liposomes was distributed in the brain efficiently.

3.10. In vivo distribution in xenografts-bearing nude mice

Distribution of CB5005-LS/DiR and LS/DiR was examined in the U87 xenografts-bearing nude mice and normal saline was used as control. Fluorescence images of nude mice at 4 h after intravenous injection demonstrated that CB5005-LS/DiR accumulated most at tumor sites and the fluorescence images of *ex vivo* xenografts were consistent with the *in vivo* result. Distribution of each formulation in the organs of the sacrificed mice including heart, liver, spleen, lung and kidney was further analyzed and the result showed relatively high accumulation of CB5005-LS/DiR and LS/DiR in liver (Fig. 5C). The quantification of fluorescence intensity in the xenografts was further conducted as shown in Fig. 5D. The fluorescence intensity of CB5005-LS/DiR-treated xenografts was significantly higher than that of LS/DiR ($p < .05$) and normal saline ($p < .001$). This result demonstrates that CB5005-LS/DiR could accumulate at tumor site after intravenous injection.

3.11. In vivo distribution in intracranial glioblastoma-bearing nude mice

Since the CB5005-modified liposome could not only penetrate into brain but also accumulate at xenograft, we are further interested whether it could accumulate in intracranial glioblastoma. Fig. 6A showed the *in vivo* images of intracranial glioblastoma-bearing nude mice at 4 h after intravenous injection of CB5005-LS/DiR, LS/DiR and normal saline, and the *ex vivo* images of dissected brains, gliomas and other organs including heart, liver, spleen, lung, and kidney. It was perspicuously observed that the fluorescence signal of CB5005-LS/DiR in the brain and glioma was much stronger than that of other groups, displaying the remarkable BBB transporting and tumor accumulating capabilities of CB5005. Undoubtedly, liver also had relatively high accumulation of liposomes as shown in Fig. 6A. Quantified fluorescence intensity of CB5005-LS/DiR-treated glioma was significantly higher than that of LS/DiR ($p < .05$) and normal saline ($p < .01$) (Fig. 6B). Furthermore, the fluorescence imaging of the brain sections showed that compared with the unmodified liposomes, fluorescence probe distributed much more in the intracranial glioblastoma when the mice were subjected to CB5005-modified liposomes administered by caudal vein injection (Fig. S2). These results indicated that CB5005 endowed the liposomes with capability of traversing BBB and accumulating in intracranial glioblastoma.

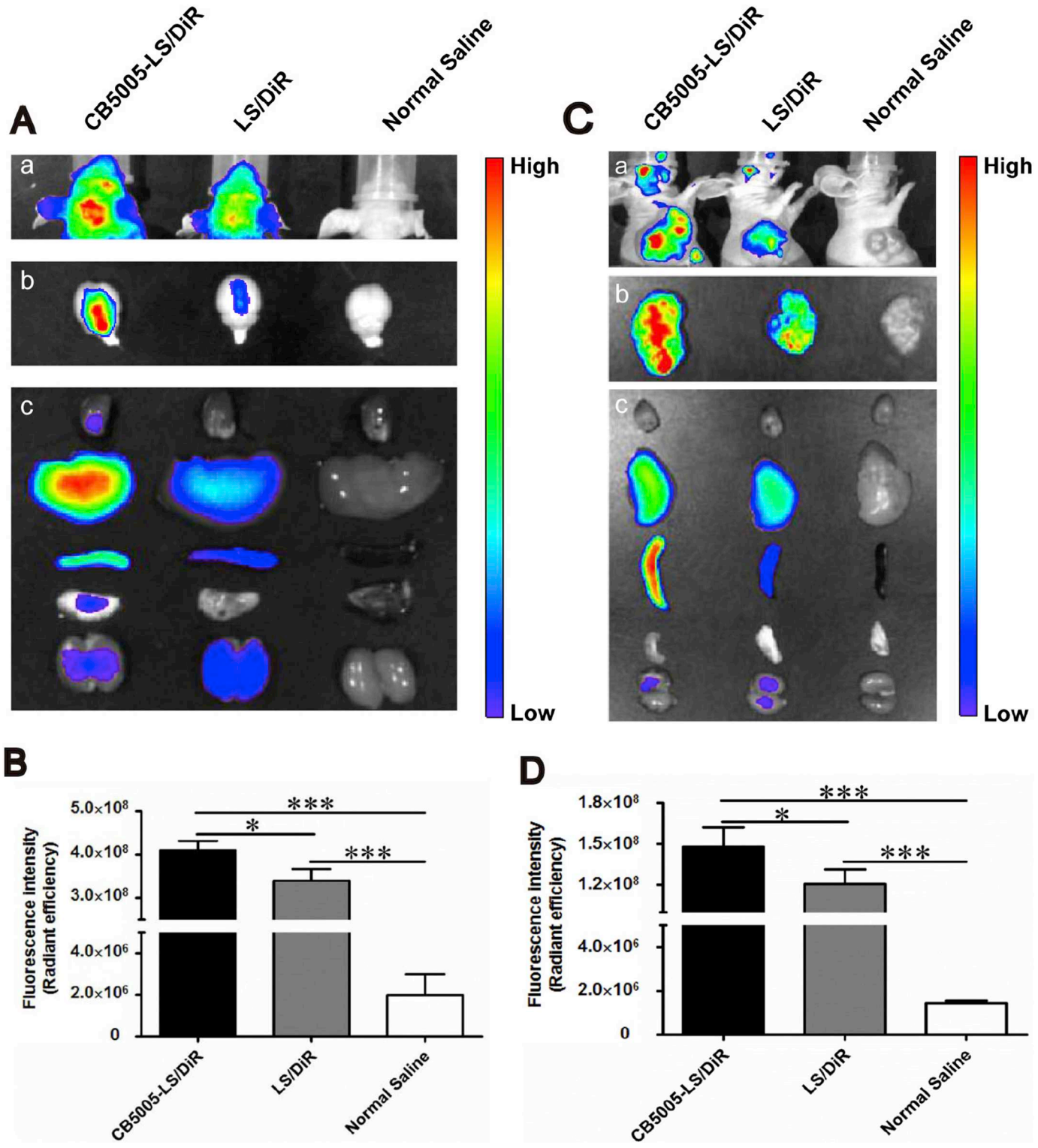

Fig. 5. *In vivo* distribution of liposomes in normal and xenografts-bearing nude mice. (A) *In vivo* distribution of CB5005-LS/DiR and LS/DiR in normal nude mice (a), and *ex vivo* distribution in brains (b) and other organs (top to bottom were heart, liver, spleen, lung and kidney) (c). From left to right, the mice were treated with CB5005-LS/DiR, LS/DiR and normal saline, respectively. The formulations were injected *via* caudal vein at a dose of 100 μL with a concentration of 0.01 μM DiR. Dissected tissues were immediately observed at 4 h post injection. (B) Quantification of fluorescence intensity in brain. Data were presented as mean ± SD ($n = 3$). * denotes statistical significance, $^{*}p < .05$, and $^{***}p < .001$. (C) *In vivo* distribution of CB5005-LS/DiR and LS/DiR in xenografts-bearing nude mice (a), and *ex vivo* distribution in xenografts (b) and other organs (top to bottom were heart, liver, spleen, lung and kidney) (c). From left to right, the mice were treated with CB5005-LS/DiR, LS/DiR and normal saline, respectively. The formulations were injected *via* caudal vein at a dose of 100 μL with a concentration of 0.01 μM DiR. Dissected tissues were immediately observed at 4 h post injection. (D) Quantification of fluorescence intensity in xenografts. Data were presented as mean ± SD (n = 3). *denotes statistical significance, $^{*}p < .05$, and $^{***}p < .001$.

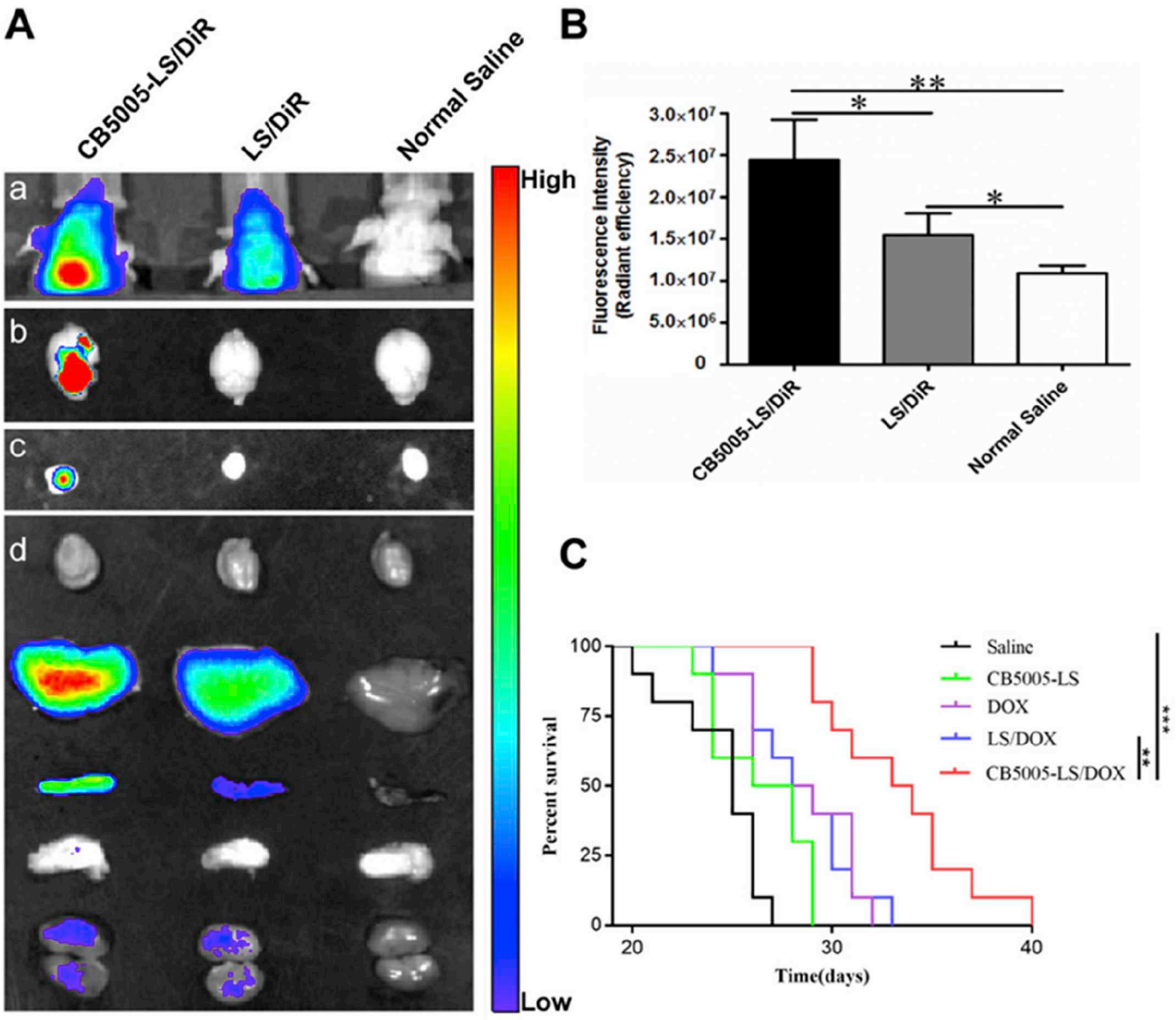

Fig. 6. *In vivo* distribution and antitumor effects of liposomes in intracranial glioblastoma-bearing nude mice. (A) The *in vivo* distribution of CB5005-LS/DiR and LS/DiR in intracranial glioblastoma-bearing nude mice (a) and the *ex vivo* distribution in brains (b), intracranial glioblastoma (c) and other organs (top to bottom were heart, liver, spleen, lung and kidney) (d). From left to right, the mice were treated with CB5005-LS/DiR, LS/DiR and normal saline, respectively. The formulations were injected *via* caudal vein at a dose of 100 μL with a concentration of 0.01 μM DiR. Dissected tissues, brain and intracranial glioblastoma were immediately observed at 4 h post injection. (B) Fluorescence intensity in intracranial glioblastoma. Data were presented as mean ± SD ($n = 3$). (C) Kaplan–Meier survival curves of nude mice bearing intracranial glioblastoma. * denotes statistical significance, $^{**}p < .01$, and $^{***}p < .001$.

3.12. Anti-glioblastoma efficacy

The anti-glioblastoma effect of CB5005-LS/DOX was demonstrated by the survival time of intracranial glioblastoma-bearing mice and the result was shown in Fig. 6C. The median survival time of CB5005-LS/DOX, LS/DOX, DOX, CB5005-LS and normal saline groups were 33.5, 28.5, 27.5, 27 and 25 days, respectively. Compared to physiological saline, CB5005-LS/DOX significantly prolonged the survival time of intracranial glioblastoma-bearing mice ($p < .001$). Also, CB5005-LS/DOX significantly prolonged the survival time when compared with LS/DOX ($p < .01$). This result indicates that CB5005-modified liposomes could enhance the inhibition efficacy of intracranial glioblastoma.

4. Discussion

Gliomas are the most primary malignant brain tumors and may occur in the brain and arise in the glial tissue [53]. Chemotherapy is considered to play an increasing important role in the treatment of gliomas. However, only about 2% of therapeutic agents can reach into the brain and much less of them can further come into contact with glioma [54]. This is because of the BBB, which acts as a physical barrier inhibiting delivery of therapeutic agents to the central nervous system and imposing obstruction for delivery of large number of drugs to pass through the endothelial capillaries to brain [55]. Tumor cell membrane is another biological barrier for delivery of therapeutic agents and their carriers [56]. Successful employment of efficient ligands, which promote accumulation of attached cargos in brain and uptake of attached cargos in glioma cells, is a point of focus in glioma chemotherapy.

Another critical problem in cancer treatment arises from drug resistance. It has been known that NF-κB could activate various genes that were involved in the development and progression of tumors, anti-apoptosis, and resistance to chemotherapy treatments [57]. High NF-κB

activity has been observed in many tumor cells including gliomas cells [58–60], which has also been confirmed in this work. Therefore, the NF-κB pathway have been targeted for treatment in both preclinical studies and clinical trials [61].

In the present study, we employed a rationally designed peptide (CB5005), which possesses dual function in cell membrane penetration and NF-κB inhibition for glioma therapy. A CB5005-conjugated liposome delivery system (CB5005-LS) was established and its cell-penetrating ability, tumor-targeting property and glioma-inhibiting efficacy were systemically investigated. Our results revealed that CB5005-conjugated liposomes could penetrate into glioma cells and tumor spheroids (Fig. 3).

Recently, various CPPs, known for their penetrating capability to brain endothelial capillaries and tumor cell membrane, have been explored for possible improvement of the efficacy of glioma therapy [12,13,62]. However, the clinical application of these cationic amino acid-based CPPs has been greatly restricted due to lack of tissue selectivity, tumor targeting ability, and *in vivo* stability as a result of high electro-positivity [63]. CPPs-conjugated cargoes would deliver the antineoplastic agents to non-target organs, which would cause adverse effects. In addition, most CPPs and their conjugated cargos distributed only in cell cytoplasm and few fluorescence-labeled cargos could be observed in cell nucleus [64].

In this study, we investigated the *in vivo* distribution of CB5005-conjugated liposomes loaded with fluorescence dye in nude mice, and our results demonstrated that they could accumulate in the brain, xenograft and even intracranial glioblastoma (Figs. 5, 6A, and Fig. S2). These interesting findings provided a solid proof that covalent conjugation of CB5005 to the liposomal surface has significantly improved BBB permeability and tumor-targeting ability of liposomes.

These results also suggested that the CB5005-LS delivery system was stable *in vivo*, which could be due to the unique hydrophobic membrane-permeable sequence of CB5005. This type of membrane translocating sequences has been utilized successfully to deliver various functional peptides and proteins into living cells [65]. In this study, the newly designed CB5005-modified liposome has shown an improved cell membrane translocating activity.

Although modification with CPP is one of the approaches to improve distribution in the brain [66,67], the mechanism of how CPP-modified nanoparticles translocate through BBB has not been fully elucidated at present. A reasonable hypothesis is CPPs might transfer across BBB *via* absorptive-mediated endocytosis (AMT) [68]. The luminal surface of cerebral endothelial cells presents an overall negative charge [69]. The positively charged CPPs are capable of penetrating lipid membranes rapidly *via* AMT and have been successfully used to bypass the P-glycoprotein in the BBB [70]. Based on this hypothesis, transport of the CB5005-modified liposomes across BBB might be also ascribed to AMT, which is triggered by electrostatic interactions between the positively charged peptide and negatively charged membrane surface regions on the brain capillary endothelial cells. The relative high concentration of negative charges on the BBB would produce a selective environment for the positively charged peptide to implement AMT [71]. Although the overall positive charge of CB5005 is not very strong under physiological conditions, it may be still sufficient to facilitate and assist the liposomes in contacting with the endothelial cells of BBB, and then the hydrophobicity of CB5005 would play a crucial role in facilitating drug delivery into the brain.

We also demonstrated that CB5005-conjugated liposomes could deliver DOX into cell nucleus (Fig. 4A and Fig. S1), which was consistent with the result from FAM-containing liposomes as shown in Fig. 3A. By contrast, liposomes without CB5005 could hardly deliver DOX into tumor cells and their nucleus. The nuclear import capability of CB5005-LS is due to the nuclear localization sequence in CB5005, which has been demonstrated by us to be effective to mediate nuclear translocation of the peptide. It was reported that nanoparticles composed of nucleolin-specific aptamers and gold nanostars could be actively transported into the nuclei of cancer cells *via* nuclear envelope invaginations. Internalization into the nuclei would not be limited by the size or shape of the nanoparticles, because it was induced by the nanoparticles outside the nuclei [72]. We suppose the CB5005-modified liposomes could also be transported into the nuclei of U87 cells by this pathway. DOX is a cytotoxic drug which acts on DNA to play its role [73,74]. Therefore, delivering DOX into cell nucleus is expected to improve the tumor-killing efficacy of DOX. We indeed demonstrated that conjugation with CB5005 could significantly improve the killing efficacy of DOX-loaded liposomes against brain tumor cells (Fig. 4B). Therefore, CB5005-conjugated liposome was an effective delivery system in the treatment of glioma.

Since CB5005-conjugated liposomes could not only distribute themselves into intracranial glioblastoma (Fig. 6A) but also deliver DOX into cell nucleus (Fig. 4A), they significantly prolonged the survival time of the mice bearing intracranial glioblastoma, compared with LS/DOX and DOX solution (Fig. 6C). The results suggested that CB5005-LS/DOX functioned through its BBB permeability, tumor targeting ability, and nuclear translocation capability. Once translocated into the tumors, CB5005 can further act as a NF-κB inhibitor to display a synergistic anti-tumor effect with DOX [33]. Therefore, CB5005-conjugated liposomes achieved the goal of overcoming sequential biological barriers and improving anti-glioma efficacy *in vivo*.

5. Conclusion

In this study, CB5005 peptide, designed as both a cell-penetrating peptide and a NF-κB inhibitor, was conjugated to PEGylated liposome for improving treatment of glioma. We demonstrated in a number of *in vitro* experiments that CB5005 modification significantly increased cellular and nuclear uptake of the liposomes by glioma cells and vastly enhance the efficacy of DOX liposomes (LS/DOX) in killing U87 tumor cells. *In vivo* imaging displayed that intravenously injected CB5005-LS distributed fluorescence dye into the brain and accumulated at xenograft and intracranial glioblastoma. As a result, dual-functional CB5005-LS/DOX significantly prolonged the survival time of nude mice bearing intracranial glioblastoma. It is anticipated that CB5005-modified liposomes would be a useful drug delivery system for chemotherapy of glioma and other human tumors.

Acknowledgment

This study was supported by the National Basic Research Program of China (973 Program, No. 2013CB932502), National Natural Science Fund of China (No. 81573358 and 8169260021), and Grants from Shanghai Science and Technology Committee, China (11431921200).

Appendix A. Supplementary data

Supplementary data to this article can be found online at https://doi.org/10.1016/j.jconrel.2018.09.016.

References

[1] P.E. Goss, K. Strasser-Weippl, B.L. Lee-Bychkovsky, L. Fan, J. Li, Y. Chavarri-Guerra, P.E. Liedke, C.S. Pramesh, T. Badovinac-Crnjevic, Y. Sheikine, Z. Chen, Y.L. Qiao, Z. Shao, L. Wu, D. Fan, L.W. Chow, J. Wang, Q. Zhang, S. Yu, G. Shen, J. He, A. Purushotham, R. Sullivan, R. Badwe, S.D. Banavali, R. Nair, L. Kumar, P. Parikh, S. Subramanian, P. Chaturvedi, S. Iyer, S.S. Shastri, R. Digumarti, E. Soto-Perez-De-Celis, D. Adilbay, V. Semiglazov, S. Orlov, D. Kaidarova, I. Tsimafeyeu, S. Tatishchev, K.D. Danishevskiy, M. Hurlbert, C. Vail, L.J. St, A. Chan, Challenges to effective cancer control in China, India, and Russia, Lancet. Oncol. 15 (2014) 489–538.

[2] R. Stupp, W.P. Mason, M.J. van den Bent, M. Weller, B. Fisher, M.J. Taphoorn, K. Belanger, A.A. Brandes, C. Marosi, U. Bogdahn, J. Curschmann, R.C. Janzer, S.K. Ludwin, T. Gorlia, A. Allgeier, D. Lacombe, J.G. Cairncross, E. Eisenhauer, R.O. Mirimanoff, Radiotherapy plus concomitant and adjuvant temozolomide for glioblastoma, N. Engl. J. Med. 352 (2005) 987–996.

[3] R. Huang, W. Ke, L. Han, J. Li, S. Liu, C. Jiang, Targeted delivery of chlorotoxin-

modified DNA-loaded nanoparticles to glioma via intravenous administration, Biomaterials 32 (2011) 2399–2406.
[4] X. Wei, J. Gao, C. Zhan, C. Xie, Z. Chai, D. Ran, M. Ying, P. Zheng, W. Lu, Liposome-based glioma targeted drug delivery enabled by stable peptide ligands, J. Control. Release 218 (2015) 13–21.
[5] H. Yan, J. Wang, P. Yi, H. Lei, C. Zhan, C. Xie, L. Feng, J. Qian, J. Zhu, W. Lu, C. Li, Imaging brain tumor by dendrimer-based optical/paramagnetic nanoprobe across the blood-brain barrier, Chem. Commun. (Camb.) 47 (2011) 8130–8132.
[6] X.Y. Li, Y. Zhao, M.G. Sun, J.F. Shi, J. Ju, C.X. Zhang, X.T. Li, W.Y. Zhao, L.M. Mu, F. Zeng, J.N. Lou, W.L. Lu, Multifunctional liposomes loaded with paclitaxel and artemether for treatment of invasive brain glioma, Biomaterials 35 (2014) 5591–604.
[7] B. Zhang, X. Sun, H. Mei, Y. Wang, Z. Liao, J. Chen, Q. Zhang, Y. Hu, Z. Pang, X. Jiang, LDLR-mediated peptide-22-conjugated nanoparticles for dual-targeting therapy of brain glioma, Biomaterials 34 (2013) 9171–9182.
[8] W.M. Pardridge, BBB-Genomics: creating new openings for brain-drug targeting, Drug Discov. Today 6 (2001) 381–383.
[9] G. Sharma, A. Modgil, B. Layek, K. Arora, C. Sun, B. Law, J. Singh, Cell penetrating peptide tethered bi-ligand liposomes for delivery to brain in vivo: biodistribution and transfection, J. Control. Release 167 (2013) 1–10.
[10] H. Liu, W. Zhang, L. Ma, L. Fan, F. Gao, J. Ni, R. Wang, The improved blood-brain barrier permeability of endomorphin-1 using the cell-penetrating peptide synB3 with three different linkages, Int. J. Pharm. 476 (2014) 1–8.
[11] L.L. Zou, J.L. Ma, T. Wang, T.B. Yang, C.B. Liu, Cell-penetrating peptide-mediated therapeutic molecule delivery into the central nervous system, Curr. Neuropharmacol. 11 (2013) 197–208.
[12] H. Yao, K. Wang, Y. Wang, S. Wang, J. Li, J. Lou, L. Ye, X. Yan, W. Lu, R. Huang, Enhanced blood-brain barrier penetration and glioma therapy mediated by a new peptide modified gene delivery system, Biomaterials 37 (2015) 345–352.
[13] M. Higa, C. Katagiri, C. Shimizu-Okabe, T. Tsumuraya, M. Sunagawa, M. Nakamura, S. Ishiuchi, C. Takayama, E. Kondo, M. Matsushita, Identification of a novel cell-penetrating peptide targeting human glioblastoma cell lines as a cancer-homing transporter, Biochem. Biophys. Res. Commun. 457 (2015) 206–212.
[14] H. Gao, Z. Yang, S. Zhang, S. Cao, Z. Pang, X. Yang, X. Jiang, Glioma-homing peptide with a cell-penetrating effect for targeting delivery with enhanced glioma localization, penetration and suppression of glioma growth, J. Control. Release 172 (2013) 921–928.
[15] K.L. Veiman, K. Kunnapuu, T. Lehto, K. Kiisholts, K. Parn, U. Langel, K. Kurrikoff, PEG shielded MMP sensitive CPPs for efficient and tumor specific gene delivery in vivo, J. Control. Release 209 (2015) 238–247.
[16] J.Y. Lee, K.H. Bae, J.S. Kim, Y.S. Nam, T.G. Park, Intracellular delivery of paclitaxel using oil-free, shell cross-linked HSA—multi-armed PEG nanocapsules, Biomaterials 32 (2011) 8635–8644.
[17] C.J. Cheng, W.M. Saltzman, Enhanced siRNA delivery into cells by exploiting the synergy between targeting ligands and cell-penetrating peptides, Biomaterials 32 (2011) 6194–6203.
[18] J. Liu, Y. Zhao, Q. Guo, Z. Wang, H. Wang, Y. Yang, Y. Huang, TAT-modified nanosilver for combating multidrug-resistant cancer, Biomaterials 33 (2012) 6155–6161.
[19] I. Nakase, Y. Konishi, M. Ueda, H. Saji, S. Futaki, Accumulation of arginine-rich cell-penetrating peptides in tumors and the potential for anticancer drug delivery in vivo, J. Control. Release 159 (2012) 181–188.
[20] P.M. Tiwari, E. Eroglu, S.S. Bawage, K. Vig, M.E. Miller, S. Pillai, V.A. Dennis, S.R. Singh, Enhanced intracellular translocation and biodistribution of gold nanoparticles functionalized with a cell-penetrating peptide (VG-21) from vesicular stomatitis virus, Biomaterials 35 (2014) 9484–9494.
[21] E. Vives, P. Brodin, B. Lebleu, A truncated HIV-1 Tat protein basic domain rapidly translocates through the plasma membrane and accumulates in the cell nucleus, J. Biol. Chem. 272 (1997) 16010–16017.
[22] S. Futaki, T. Suzuki, W. Ohashi, T. Yagami, S. Tanaka, K. Ueda, Y. Sugiura, Arginine-rich peptides. An abundant source of membrane-permeable peptides having potential as carriers for intracellular protein delivery, J. Biol. Chem. 276 (2001) 5836–5840.
[23] E. Vives, J. Schmidt, A. Pelegrin, Cell-penetrating and cell-targeting peptides in drug delivery, Biochim. Biophys. Acta 1786 (2008) 126–138.
[24] P. Jarver, U. Langel, Cell-penetrating peptides—a brief introduction, Biochim. Biophys. Acta 1758 (2006) 260–263.
[25] D.S. Liang, H.T. Su, Y.J. Liu, A.T. Wang, X.R. Qi, Tumor-specific penetrating peptides-functionalized hyaluronic acid-d-alpha-tocopheryl succinate based nanoparticles for multi-task delivery to invasive cancers, Biomaterials 71 (2015) 11–23.
[26] S. Kameyama, M. Horie, T. Kikuchi, T. Omura, T. Takeuchi, I. Nakase, Y. Sugiura, S. Futaki, Effects of cell-permeating peptide binding on the distribution of 125I-labeled Fab fragment in rats, Bioconjug. Chem. 17 (2006) 597–602.
[27] D. Fischer, Y. Li, B. Ahlemeyer, J. Krieglstein, T. Kissel, In vitro cytotoxicity testing of polycations: influence of polymer structure on cell viability and hemolysis, Biomaterials 24 (2003) 1121–1131.
[28] S. Li, W.C. Tseng, D.B. Stolz, S.P. Wu, S.C. Watkins, L. Huang, Dynamic changes in the characteristics of cationic lipidic vectors after exposure to mouse serum: implications for intravenous lipofection, Gene Ther. 6 (1999) 585–594.
[29] H. Eliyahu, N. Servel, A.J. Domb, Y. Barenholz, Lipoplex-induced hemagglutination: potential involvement in intravenous gene delivery, Gene Ther. 9 (2002) 850–858.
[30] B.R. Liu, Y.W. Huang, J.G. Winiarz, H.J. Chiang, H.J. Lee, Intracellular delivery of quantum dots mediated by a histidine- and arginine-rich HR9 cell-penetrating peptide through the direct membrane translocation mechanism, Biomaterials 32 (2011) 3520–3537.
[31] S. Katayama, H. Hirose, K. Takayama, I. Nakase, S. Futaki, Acylation of octaarginine: implication to the use of intracellular delivery vectors, J. Control. Release 149 (2011) 29–35.
[32] P.A. Wender, W.C. Galliher, E.A. Goun, L.R. Jones, T.H. Pillow, The design of guanidinium-rich transporters and their internalization mechanisms, Adv. Drug Deliv. Rev. 60 (2008) 452–472.
[33] L. Zhang, Y. Zhang, L. Tai, K. Jiang, C. Xie, Z. Li, Y.Z. Lin, G. Wei, W. Lu, W. Pan, Functionalized cell nucleus-penetrating peptide combined with doxorubicin for synergistic treatment of glioma, Acta Biomater. 42 (2016) 90–101.
[34] Y.Z. Lin, S.Y. Yao, R.A. Veach, T.R. Torgerson, J. Hawiger, Inhibition of nuclear translocation of transcription factor NF-kappa B by a synthetic peptide containing a cell membrane-permeable motif and nuclear localization sequence, J. Biol. Chem. 270 (1995) 14255–14258.
[35] C.F. Chian, C.H. Chiang, C.H. Chuang, S.L. Liu, Inhibitor of nuclear factor-kappaB, SN50, attenuates lipopolysaccharide-induced lung injury in an isolated and perfused rat lung model, Transl. Res. 163 (2014) 211–220.
[36] L. Catrysse, G. van Loo, Inflammation and the Metabolic Syndrome: the Tissue-specific Functions of NF-kappaB, Trends Cell Biol. 27 (2017) 417–429.
[37] M.S. Hayden, S. Ghosh, Shared principles in NF-kappaB signaling, Cell 132 (2008) 344–362.
[38] Q. Zhang, M.J. Lenardo, D. Baltimore, 30 years of NF-kappaB: a blossoming of relevance to human pathobiology, Cell 168 (2017) 37–57.
[39] K. Taniguchi, M. Karin, NF-kappaB, inflammation, immunity and cancer: coming of age, Nat. Rev. Immunol. 18 (2018) 309–324.
[40] M. Boothby, Specificity of sn50 for NF-kappa B? Nat. Immun. 2 (2001) 471–472.
[41] H.S. Qhattal, T. Hye, A. Alali, X. Liu, Hyaluronan polymer length, grafting density, and surface poly(ethylene glycol) coating influence in vivo circulation and tumor targeting of hyaluronan-grafted liposomes, ACS Nano 8 (2014) 5423–5440.
[42] E. Vacas-Cordoba, M. Galan, F.J. de la Mata, R. Gomez, M. Pion, M.A. Munoz-Fernandez, Enhanced activity of carbosilane dendrimers against HIV when combined with reverse transcriptase inhibitor drugs: searching for more potent microbicides, Int. J. Nanomedicine 9 (2014) 3591–3600.
[43] P.M. Valencia, P.A. Basto, L. Zhang, M. Rhee, R. Langer, O.C. Farokhzad, R. Karnik, Single-step assembly of homogenous lipid-polymeric and lipid-quantum dot nanoparticles enabled by microfluidic rapid mixing, ACS Nano 4 (2010) 1671–1679.
[44] K.A. Gregersen, Z.B. Hill, J.C. Gadd, B.S. Fujimoto, D.J. Maly, D.T. Chiu, Intracellular delivery of bioactive molecules using light-addressable nanocapsules, ACS Nano 4 (2010) 7603–7611.
[45] P.P. Deshpande, S. Biswas, V.P. Torchilin, Current trends in the use of liposomes for tumor targeting, Nanomed. (Lond) 8 (2013) 1509–1528.
[46] T. Jiang, Z. Zhang, Y. Zhang, H. Lv, J. Zhou, C. Li, L. Hou, Q. Zhang, Dual-functional liposomes based on pH-responsive cell-penetrating peptide and hyaluronic acid for tumor-targeted anticancer drug delivery, Biomaterials 33 (2012) 9246–9258.
[47] Y. Ding, D. Sun, G.L. Wang, H.G. Yang, H.F. Xu, J.H. Chen, Y. Xie, Z.Q. Wang, An efficient PEGylated liposomal nanocarrier containing cell-penetrating peptide and pH-sensitive hydrazone bond for enhancing tumor-targeted drug delivery, Int. J. Nanomedicine 10 (2015) 6199–6214.
[48] Z. Yan, F. Wang, Z. Wen, C. Zhan, L. Feng, Y. Liu, X. Wei, C. Xie, W. Lu, LyP-1-conjugated PEGylated liposomes: a carrier system for targeted therapy of lymphatic metastatic tumor, J. Control. Release 157 (2012) 118–125.
[49] M. Ying, Q. Shen, Y. Liu, Z. Yan, X. Wei, C. Zhan, J. Gao, C. Xie, B. Yao, W. Lu, Stabilized heptapeptide A7R for enhanced multifunctional liposome-based tumor-targeted drug delivery, Acs Appl. Mater. Inter. 8 (2016) 13232–13241.
[50] G. Haran, R. Cohen, L.K. Bar, Y. Barenholz, Transmembrane ammonium sulfate gradients in liposomes produce efficient and stable entrapment of amphipathic weak bases, Biochim. Biophys. Acta 1151 (1993) 201–215.
[51] J. Shen, C. Zhan, C. Xie, Q. Meng, B. Gu, C. Li, Y. Zhang, W. Lu, Poly(ethylene glycol)-block-poly(D,L-lactide acid) micelles anchored with angiopep-2 for brain-targeting delivery, J. Drug Traget 19 (2011) 197–203.
[52] J.M. Garner, M. Fan, C.H. Yang, Z. Du, M. Sims, A.M. Davidoff, L.M. Pfeffer, Constitutive activation of signal transducer and activator of transcription 3 (STAT3) and nuclear factor kappaB signaling in glioblastoma cancer stem cells regulates the Notch pathway, J. Biol. Chem. 288 (2013) 26167–26176.
[53] Q.T. Ostrom, L. Bauchet, F.G. Davis, I. Deltour, J.L. Fisher, C.E. Langer, M. Pekmezci, J.A. Schwartzbaum, M.C. Turner, K.M. Walsh, M.R. Wrensch, J.S. Barnholtz-Sloan, The epidemiology of glioma in adults: a “state of the science” review, Neuro-Oncology 16 (2014) 896–913.
[54] J. Cote, V. Bovenzi, M. Savard, C. Dubuc, A. Fortier, W. Neugebauer, L. Tremblay, W. Muller-Esterl, A.M. Tsanaclis, M. Lepage, D. Fortin, F.J. Gobeil, Induction of selective blood-tumor barrier permeability and macromolecular transport by a biostable kinin B1 receptor agonist in a glioma rat model, PLoS One 7 (2012) e37485.
[55] R.K. Upadhyay, Drug delivery systems, CNS protection, and the blood brain barrier, Biomed. Res. Int. 2014 (2014) 869269.
[56] M.H. Kang, M.J. Park, H.J. Yoo, K.Y. Hyuk, S.G. Lee, S.R. Kim, D.W. Yeom, M.J. Kang, Y.W. Choi, RIPL peptide (IPLVVPLRRRRRRRRC)-conjugated liposomes for enhanced intracellular drug delivery to hepsin-expressing cancer cells, Eur. J. Pharm. Biopharm. 87 (2014) 489–499.
[57] N.D. Perkins, The diverse and complex roles of NF-kappaB subunits in cancer, Nat. Rev. Cancer 12 (2012) 121–132.
[58] V.T. Puliyappadamba, K.J. Hatanpaa, S. Chakraborty, A.A. Habib, The role of NF-kappaB in the pathogenesis of glioma, Mol. Cell Oncol. 1 (2014) e963478.
[59] X. Wang, L. Jia, X. Jin, Q. Liu, W. Cao, X. Gao, M. Yang, B. Sun, NF-kappaB inhibitor reverses temozolomide resistance in human glioma TR/U251 cells, Oncol. Lett. 9 (2015) 2586–2590.
[60] J.A. Didonato, F. Mercurio, M. Karin, NF-kappaB and the link between inflammation and cancer, Immunol. Rev. 246 (2012) 379–400.

[61] D. Nagel, M. Vincendeau, A.C. Eitelhuber, D. Krappmann, Mechanisms and consequences of constitutive NF-kappaB activation in B-cell lymphoid malignancies, Oncogene 33 (2014) 5655–5665.
[62] F. Zhang, C.L. Xu, C.M. Liu, Drug delivery strategies to enhance the permeability of the blood-brain barrier for treatment of glioma, Drug Des. Devel. Ther. 9 (2015) 2089–2100.
[63] E. Koren, V.P. Torchilin, Cell-penetrating peptides: breaking through to the other side, Trends Mol. Med. 18 (2012) 385–393.
[64] J.M. Steinbach, Y.E. Seo, W.M. Saltzman, Cell penetrating peptide-modified poly (lactic-co-glycolic acid) nanoparticles with enhanced cell internalization, Acta Biomater. 30 (2016) 49–61.
[65] M. Rojas, J.P. Donahue, Z. Tan, Y.Z. Lin, Genetic engineering of proteins with cell membrane permeability, Nat. Biotechnol. 16 (1998) 370–375.
[66] T.T. Zhang, W. Li, G. Meng, P. Wang, W. Liao, Strategies for transporting nanoparticles across the blood-brain barrier, Biomater. Sci. 4 (2016) 219–229.
[67] R. Alyautdin, I. Khalin, M.I. Nafeeza, M.H. Haron, D. Kuznetsov, Nanoscale drug delivery systems and the blood-brain barrier, Int. J. Nanomedicine 9 (2014) 795–811.
[68] Y. Qin, H. Chen, W. Yuan, R. Kuai, Q. Zhang, F. Xie, L. Zhang, Z. Zhang, J. Liu, Q. He, Liposome formulated with TAT-modified cholesterol for enhancing the brain delivery, Int. J. Pharm. 419 (2011) 85–95.
[69] F. Herve, N. Ghinea, J.M. Scherrmann, CNS delivery via adsorptive transcytosis, AAPS J. 10 (2008) 455–472.
[70] Y. Liu, L. Mei, Q. Yu, C. Xu, Y. Qiu, Y. Yang, K. Shi, Q. Zhang, H. Gao, Z. Zhang, Q. He, Multifunctional tandem peptide modified paclitaxel-loaded liposomes for the treatment of vasculogenic mimicry and cancer stem cells in malignant glioma, ACS Appl. Mater. Interfaces 7 (2015) 16792–16801.
[71] H. Xia, X. Gao, G. Gu, Z. Liu, Q. Hu, Y. Tu, Q. Song, L. Yao, Z. Pang, X. Jiang, J. Chen, H. Chen, Penetratin-functionalized PEG-PLA nanoparticles for brain drug delivery, Int. J. Pharm. 436 (2012) 840–850.
[72] D.H. Dam, J.H. Lee, P.N. Sisco, D.T. Co, M. Zhang, M.R. Wasielewski, T.W. Odom, Direct observation of nanoparticle-cancer cell nucleus interactions, ACS Nano 6 (2012) 3318–3326.
[73] S. Imstepf, V. Pierroz, P. Raposinho, M. Felber, T. Fox, C. Fernandes, G. Gasser, I.R. Santos, R. Alberto, Towards (99m)Tc-based imaging agents with effective doxorubicin mimetics: a molecular and cellular study, Dalton Trans. 45 (2016) 13025–13033.
[74] Z. Farhane, F. Bonnier, M.A. Maher, J. Bryant, A. Casey, H.J. Byrne, Differentiating responses of lung cancer cell lines to Doxorubicin exposure: in vitro Raman micro spectroscopy, oxidative stress and bcl-2 protein expression, J. Biophotonics. 10 (2017) 151–165.